

# Thermal expansion of $\text{CaIrO}_3$ post-perovskite determined by time-of-flight measurements

F. Aguado,<sup>1</sup> S. Hirai,<sup>2</sup> S. A. T. Redfern,<sup>3</sup> R. I. Smith<sup>4</sup>

<sup>1</sup>MALTA-Consolider team. Unidad Asociada ICMA-CSIC. DCITIMAC, Universidad de Cantabria, 39005-Cantabria, Spain

<sup>2</sup>Department of Geological & Environmental Sciences, Stanford University, Stanford CA 94305-2115, USA

<sup>3</sup>Department of Earth Sciences, University of Cambridge, Cambridge CB2 3EQ, UK

<sup>4</sup>Rutherford Appleton Lab, ISIS facility, Didcot OX11 0QX, UK

Email:aguadof@unican.es

**Abstract.** The thermal evolution of the  $\text{CaIrO}_3$  post-perovskite structure has been determined by neutron powder diffraction (time-of-flight) measurements in a wide temperature range, from 1.8K to 550K. The linear expansion is similar to that found in previous x-ray diffraction studies, being  $\alpha_b > \alpha_c > \alpha_a$ . However, the difference in relative lattice parameters is less pronounced in the present case, suggesting a more isotropic evolution under temperature. Other structural differences found at low and high temperatures through several X-ray and neutron diffraction studies have been also analysed.

## 1. Introduction

Recent studies on different perovskites ( $pv$ ) constituting the Earth's mantle revealed a new denser structure under extreme conditions.<sup>1</sup> This arrangement found in  $\text{MgSiO}_3$  at high pressures and temperatures, i.e. the post-perovskite ( $ppv$ ) phase, is the same as that seen in  $\text{CaIrO}_3$  at room conditions: a layered structure of  $\text{IrO}_6$  octahedra sharing corners and edges along different crystallographic directions within the plane (see fig. 1).<sup>2</sup> Accordingly,  $\text{CaIrO}_3$  was initially proposed to carry out studies on compression at moderate P/T, being a good analogue for understanding the structural behaviour of the unquenchable  $\text{MgSiO}_3$   $ppv$  phase.<sup>3</sup> However, later reports challenged the suitability of  $\text{CaIrO}_3$  to describe elastic properties of silicates at lower mantle conditions.<sup>4</sup> In addition, recent studies on isostructural compounds show different compression and expansion trends depending on the system.<sup>5</sup> Consequently, there is still an intense activity devoted to explain the deformation mechanisms found in this kind of compounds, which is particularly interesting to rationalize the structural behaviour of the  $\text{ABX}_3$  family. Since  $\text{ASiO}_3$  compounds are the main mantle constituents, it is especially important to clarify their behaviour at the mantle-core interface, i.e. the D'' layer, crucial to understand the seismic features found at that level.

$\text{CaIrO}_3$  can be isolated in either the  $pv$  or the  $ppv$  phase, just modifying the synthesis conditions. The  $ppv$  phase has been proved to be stable in wide pressure and temperature ranges.<sup>6,7</sup> However, concerning temperature solely, significant differences can be found in structures from different reports.<sup>7-9</sup> In addition, a full structural characterization in a wide temperature range hasn't been performed yet. Therefore, before analysing complex high P/T behaviours, it is important to properly determine the temperature effect on  $\text{CaIrO}_3$   $ppv$  structure.



Here we report the structural evolution of  $\text{CaIrO}_3$ -*ppv* in the 1.8-550 K range determined from time-of-flight (TOF) measurements on powder samples synthesized at high P/T. Thermal expansion results will be compared to available data from XRD and neutron diffraction experiments on samples obtained from different methods.

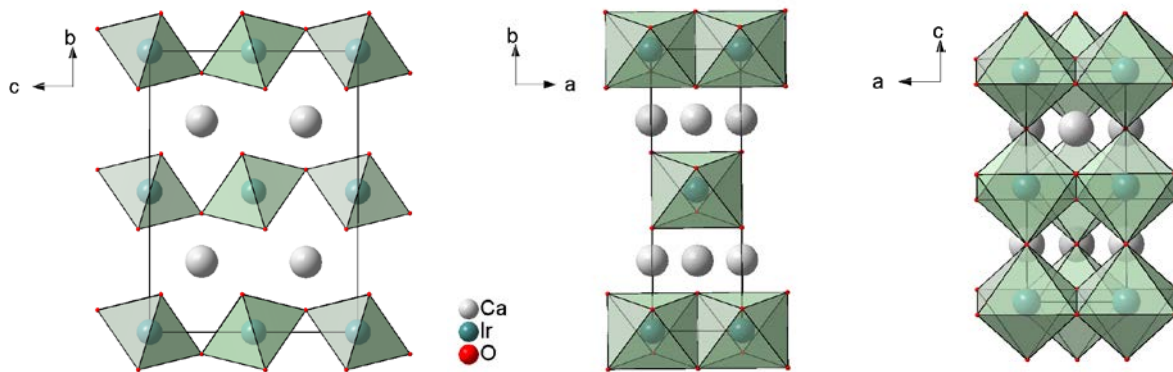


**Figure 1** Views of the layered  $\text{CaIrO}_3$  post-perovskite structure along the *a*, *c* and *b* axes.

## 2. Experimental

$\text{CaIrO}_3$  powder samples were obtained through high P/T synthesis by using a piston-cylinder apparatus. Stoichiometric amounts of starting oxides ( $\text{IrO}_2$  and  $\text{CO}$ ) were thermally pretreated and subsequently loaded in a graphite furnace-type assembly with a talc-pyrex outer sleeve. Different applied pressures (0.9-2.5 GPa), temperatures (1275K-1675K) and treatment durations (30 min-2hrs.) were explored, determining the optimal conditions to avoid  $\text{Ca}_2\text{IrO}_4$  and  $\text{CaIrO}_3$ -*pv* in the final product. Thus, quenched samples showed no significant traces of such phases through XRD analysis. TOF neutron powder diffraction experiments (NPD) were carried out at the POLARIS instrument, ISIS facility. Given the limited sample amount and the strong iridium absorption, some pellets were loaded in a low signal vanadium can and placed in a standard cryofurnace. Several patterns were recorded in the 1.8K- 550K range, with counting times ranging from 7 h to 8h. Prior to any analysis, data were corrected for absorption to get appropriate intensities for full structural characterization. Subsequently, data from the highest resolution detector were used to perform full Rietveld refinements by means of the GSAS package.<sup>10</sup>

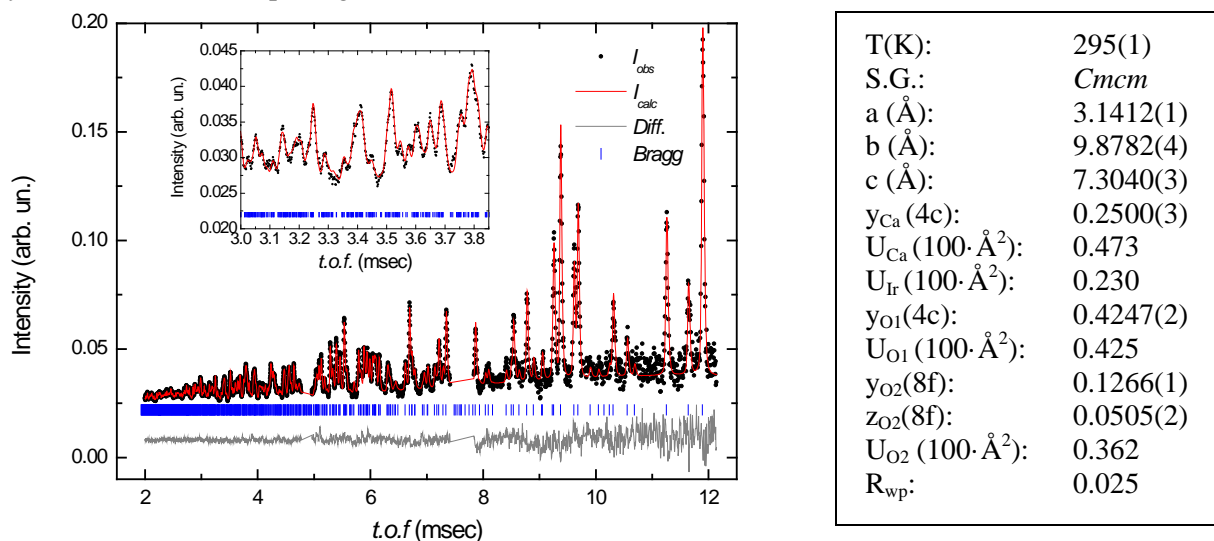


**Figure 2** Results of Rietveld refinement of  $\text{CaIrO}_3$  at  $T=295$  K. Note that other  $a_i=0$  except  $z_{\text{O1}}=1/4$ .

### 3. Results and discussion

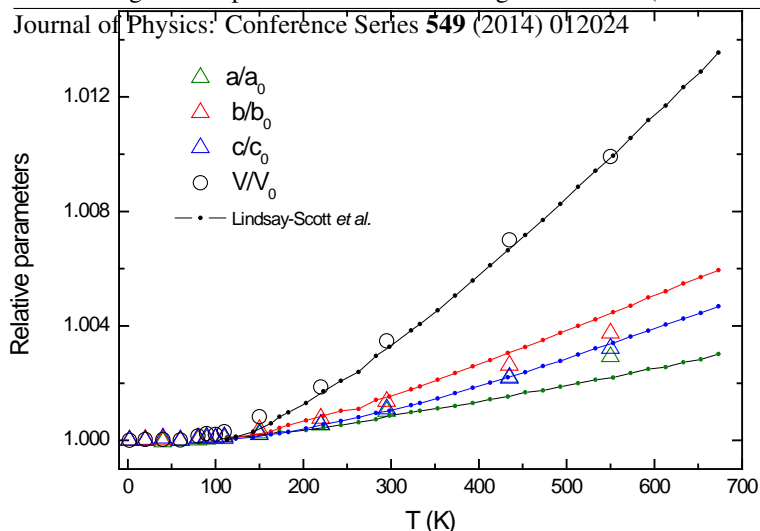
Rietveld refinements were carried out using the centrosymmetric Space Group  $Cmcm$ , which provided the best agreement factors. Thus, the use of the alternative non-centrosymmetric  $Cmc2_1$  group is not justified.<sup>2,9</sup> Apart from the crystal  $ppv$  phase, no additional contributions (impurities or magnetic phases) were detected in any of the patterns within the experimental error. Figure 2 shows the results of the structural analysis at ambient temperature. Refined lattice parameters, the four non-special atomic positions and the isotropic temperature factors are included in the table. The structure is compatible with previous diffraction experiments.<sup>2,7-9</sup> It can be rationalized as a series of layers along the crystallographic  $b$  direction, formed by interconnected  $IrO_6$  octahedra, sharing edges and corners along the  $a$  and  $c$  directions, respectively (see fig. 1). The Ir-O bond lengths (1.970Å and 2.040Å) and the Ir-O1-Ir tilting angle ( $\theta = 135.8^\circ$ ) are very close to available values on single crystal and powder samples from ambient pressure synthesis.<sup>2</sup>

Table 1 includes a summary of results on the  $CaIrO_3$  structure at selected low and high temperatures, comparing lattice from different reports (NPD and XRD). Thus, differences in lattice parameters and volumes within the same range are below 0.3% and 0.1%, respectively, whereas in the unit cell ratios are lower than 0.5% (the biggest discrepancies corresponding to RT). However, in spite of the small differences between them, it is necessary to carefully analyse their temperature evolution.

**Table 1.** Lattice parameters and unit cell metrics determined at selected temperatures for  $CaIrO_3$ .

	$\approx 2\text{ K}$		RT			$\approx 550\text{ K}$		
	This study	Ref. 9	This study	Ref. 9	Ref. 7	This study	Ref. 6	Ref. 7
	NPD	NPD	NPD	NPD	XRD	NPD	XRD	XRD
$a$ (Å)	3.1374	3.1345	3.1406	3.1365	3.1457	3.1466	3.1447	3.1499
$b$ (Å)	9.8631	9.8757	9.8764	9.8835	9.8640	9.9000	9.9055	9.8932
$c$ (Å)	7.2948	7.2952	7.3028	7.2990	7.2975	7.3183	7.3147	7.3148
$V$ (Å <sup>3</sup> )	225.73	225.83	226.52	226.26	226.44	227.97	227.95	227.95
$b/a$	3.144	3.151	3.145	3.151	3.136	3.146	3.150	3.141
$c/a$	2.325	2.327	2.325	2.327	2.320	2.326	2.326	2.322
T (K)	1.8	2.0	295	293	298	550	536	553

Figure 3 shows the relative lattice parameters and cell volume as a function of temperature in the 1.8- 550 K range. Previous data from Lindsay-Scott *et al.* (XRD)<sup>7</sup> have been included for comparison purposes. It can be observed that the expansion is anisotropic in both cases, although differences are much less pronounced in the present study. In both cases the  $b$  axis shows the greatest variation, that is, the interlayer expands more than any of the intralayer distances. In addition,  $a$  and  $c$  relative variations are quite similar, being the former (the edge-sharing direction) slightly smaller. Thus, results from thermal expansion indicate that  $\alpha_b > \alpha_c > \alpha_a$ . Interestingly, the pressure effect on lattice anisotropy is not exactly the opposite of thermal expansion, as one could expect: The  $a$  axis compresses less than the  $c$  axis, being  $\beta_c > \beta_a > \beta_b$ .<sup>8,11</sup> However their relative variation is quite similar, representing only 0.1% between 0 and 8 GPa, whereas  $\Delta b$  is approximately 1% over the  $a$  and  $c$  average in the same pressure range. This result agrees well with the rather isotropic expansion observed in the  $a$ - $c$  plane through the present study. On the contrary, the isostructural  $MgSiO_3$  presents



**Figure 3.** Temperature dependence of the relative volume and lattice parameters. Data from ref. 7 is also included for comparison.

a regular behaviour in this respect, showing  $\alpha_i$  and  $1/\beta_i$  the same sequence.<sup>12</sup> Nevertheless, the greatest expansion still corresponds to the interlayer direction ( $\alpha_b > \alpha_a > \alpha_c$ ), unlike some results observed in the  $\text{CaBO}_3$  family, where more differences can be found among *ppv* analogues. Thus, the expansion in  $\text{CaPtO}_3$  differs from that of  $\text{CaIrO}_3$  and  $\text{MgSiO}_3$ , being  $\alpha_c > \alpha_b > \alpha_a$ , whereas on compression the anisotropy is the same:  $\beta_c > \beta_a > \beta_b$ .<sup>5</sup> In  $\text{CaRhO}_3$  the variation of the *c* axis is also the greatest,  $\alpha_c > \alpha_a > \alpha_b$ , decreasing the interlayer distance (*b* axis) monotonically above the magnetic phase transition ( $T_N = 90\text{K}$ ).<sup>13</sup> Finally,  $\text{CaRuO}_3$  presents a slight reduction of the *a* axis as temperature increases, as well as the same expansion sequence as in  $\text{CaIrO}_3$ :  $\alpha_b > \alpha_c > \alpha_a$ .<sup>14</sup> This plethora of thermal behaviours among analogues foresees a complex explanation of expansion systematics within the *ppv* family.

#### 4. Conclusions

The thermal evolution of  $\text{CaIrO}_3$  *ppv* structure has been established through a TOF experiment conducted at the ISIS facility. In the 1.8-550K range the *Cmcm* structure is stable and no additional phases were detected below the magnetic ordering temperature ( $T_C = 108\text{K}$ ).<sup>2</sup> The thermal expansion is similar to that reported in literature, with  $\alpha_b > \alpha_c > \alpha_a$ , although significant quantitative differences have been found, being the expansion considerably more isotropic than previously reported. Nevertheless, discrepancies could be associated to sample synthesis procedure and additional experiments are required to unambiguously determine the source of such differences. The thermal behaviour within the  $\text{CaBO}_3$  family is rather complex and, consequently, especial attention must be paid when dealing with such compounds as  $\text{MgSiO}_3$  *ppv* analogues.

#### References

- [1] Murakami M, Hirose K, Kawamura K, Sata N and Ohishi Y 2004 *Science* **304** 855.
- Oganov A R and Ono S 2004 *Nature* **430** 445.
- [2] Hirai S, Welch M D, Aguado F and Redfern S A T 2009, *Z. Kristallog.* **224** 345.
- Hirai S *et al.* 2011 *Chem. Mat.* **23** 119.
- [3] Hirose K and Fujita Y 2005 *Geophys. Res. Lett.* **32** L13313.
- [4] Niwa K, Yagi T and Ohgushi K 2011 *Phys. Chem. Minerals* **38** 21.
- [5] Lindsay-Scott A *et al.* 2011 *J. Appl. Cryst.* **44** 999.
- [6] Liu W *et al.* 2011 *Phys. Chem. Minerals* **38** 407.
- [7] Lindsay-Scott A, Wood I G and Dobson D P 2007 *PEPI* **162** 140.
- [8] Martin C D *et al.* 2007 *American Mineral.* **92** 1048.
- [9] Martin C D *et al.* 2007 *American Mineral.* **92** 1912.
- [10] Larson A C and Von Dreele R B 2000 *Los Alamos National Laboratory Report LAUR* **86** 748.
- [11] Boffa Ballaran T, Trønnes R G and Frost D J 2007 *American Mineral.* **92** 176.
- [12] Guignot N *et al.* 2007 *Earth Planet. Sci. Lett.* **256**, 162.
- [13] Wang X X *et al.* 2011 *Physica C* **471** 763.
- [14] Shirako Y *et al.* 2011 *Phys. Rev. B* **83** 174411.